ELSEVIER

Chemical Engineering Journal 90 (2002) 231–240

Chemical Engineering Journal

www.elsevier.com/locate/cej

# Two-layer shrinking-core model: parameter estimation for the reaction order in leaching processes

Antonio Velardo [a], Massimiliano Giona [a,*], Alessandra Adrover [a], Francesca Pagnanelli [b], Luigi Toro [b]

[a] *Facolta di Ingegneria, Dipartimento di Ingegneria Chimica, Universitá di Roma "La Sapienza", via Eudossiana 18, 00184 Rome, Italy*
[b] *Dipartimento di Chimica, Universitá di Roma "La Sapienza", Piazzale Aldo Moro 5, 00185 Rome, Italy*

Received 10 December 2001; accepted 23 February 2002

**Abstract**

This article develops a modified version of the shrinking-core model accounting for the surface heterogeneity of solid particles. This model can be primarily used as a shortcut method for estimating the dependence of the kinetic rates on the concentration of fluid reactants and specifically the reaction order in the presence of a polydisperse solid mixture. This approach is tested numerically for model reactions involving polydisperse systems and is applied to the dissolution of $MnO_2$ in sulphuric acid solutions containing glucose as the reductant agent.


*Keywords:* Two-layer shrinking-core model; Surface heterogeneity; Polydisperse systems

## 1. Introduction

Dissolution kinetics of solid particles and leaching processes are typical industrially relevant operations, for which the structural properties of the solid particles influence significantly the reaction evolution and its optimization [1,2]. As a consequence, scale-up of process units may be particularly difficult.

Dissolution kinetics depends on four major effects: (i) the reaction kinetics sensu stricto and, specifically, the dependence of the dissolution rates on the concentration of fluid reactants; (ii) transport effects and mass transfer limitations; (iii) the structural properties of particle ensembles expressed by the particle distribution function [3–7]; (iv) the mechanical/dissolution effects leading to particle fragmentation and break-up induced either by the mechanical stirring or by the dissolution kinetics itself [8,9]. The latter two effects depend on the polydispersity of the mixture and influence the dynamics of the particle distribution function during the process.

From these general observations, it follows that an accurate description of dissolution phenomena and their scale-up from laboratory to industrial equipment, cannot be grounded solely on shrinking-core models, which intrinsically overlook the polydispersity of the solid particle ensemble. Conversely, structured models expressed by means of population balances are one of the most powerful tools to approach these processes [10]. For batch dissolution kinetics, population balance models are expressed mathematically by means of a non-linear integral–differential equation for the particle distribution function $n(r, t)$:

$$\frac{\partial n(r,t)}{\partial t} + \frac{\partial}{\partial r}\{\omega[r, N_3(t)]n(r,t)\} = -a(r)n(r,t) + \int_0^\infty a(\rho)b(r;\rho)n(\rho,t)\,\mathrm{d}\rho, \tag{1.1}$$

where $n(r, t)\,\mathrm{d}r$ is the number of solid particles with radius between $r$ and $r+\mathrm{d}r$. The function $a(r)$ is the fragmentation rate and $b(r;\rho)$ expresses the number of fragments of radius $r$ generated from a particle of radius $\rho$. By definition, the kernel $b(r;\rho)$ satisfies the constraint $b(r;\rho) = 0$, for $\rho < r$ and the mass conservation condition [8,9]:

$$\rho^3 = \int_0^\rho r^3 b(r;\rho)\,\mathrm{d}r. \tag{1.2}$$

The dissolution rate $\omega[r, N_3(t)]$, that is:

$$\frac{\mathrm{d}r}{\mathrm{d}t} = \omega[r, N_3(t)], \tag{1.3}$$

is a non-linear integral functional of the particle distribution function $n(r, t)$, since it may depend explicitly on its third-order moment:

$$N_3(t) = \int_0^\infty r^3 n(r,t)\,\mathrm{d}r. \tag{1.4}$$

* Corresponding author. Tel.: +39-6-445-85-892; fax: +39-6-445-85-339.
*E-mail address:* max@giona.ing.uniroma1.it (M. Giona).

1385-8947/02/$ – see front matter 
PII: S1385-8947(02)00038-4

**Nomenclature**

| | |
|---|---|
| $a(r)$ | fragmentation rate |
| $b(r, \rho)$ | number of fragments of radius $r$ generated by a particle of radius $\rho$ |
| $c_i$ | molar concentration of the $i$th fluid reactant |
| $c_{s,0}$ | $n_{s,0}/V_r$ |
| $d$ | distance function defined by Eq. (4.5) |
| $k_0$ | dissolution rate pre-factor |
| $k_d$ | $k_0 c_{s,0}^{n_1+n_2}$ |
| $n_i$ | reaction order with respect of the $i$th fluid reactant |
| $n(r, t)$ | particle distribution function |
| $n_{s,0}$ | moles of solid reactant initially present |
| $N_k$ | $k$th order moment of the particle distribution function |
| $r$ | radius |
| $R_i$ | internal core radius |
| $R_{max}$ | upper bound for the particle radius of a polydisperse mixture |
| $R_o$ | external particle radius |
| $S$ | particle surface |
| $S_{eff}$ | effective particle surface |
| $t$ | time |
| $T$ | temperature |
| $V$ | particle volume |
| $V_r$ | reactor volume |
| $x$ | dimensionless radius |
| $X$ | conversion |

*Greek letters*

| | |
|---|---|
| $\alpha$ | surface heterogeneity factor |
| $\beta$ | steepness factor |
| $\gamma_i$ | loading ratio $c_i(0)/c_{s,0}\nu_i$ |
| $\theta$ | dimensionless time |
| $\nu_i$ | stoichiometric coefficient of the $i$th fluid species |
| $\phi(r; R_i, R_o)$ | modulation function, Eq. (3.6) |
| $\omega$ | dissolution rate |

The functional form $\omega = \omega[r, N_3(t)]$ accounts for the dependence of the dissolution rate on the concentration of the fluid reactants within the fluid phase, under the hypothesis of perfectly mixed conditions and is a straightforward consequence of the stoichiometric constraints (see Section 4 for further details). The dependence of $\omega$ on $r$ is a consequence of the interplay between the kinetics of dissolution and mass transfer limitations [6].

The functional (non-linear integral–differential) form of the population balance equation Eq. (1.1) indicates that it is extremely difficult to decouple the kinetic effects from the structural properties associated with mixture polydispersity and fragmentation dynamics. Consequently, the estimation of all the parameters, functions and kernels entering Eq. (1.1) should be based on physical approximations aimed at simplifying the numerical approach, so as to reduce the problem to a series of subtasks that are easier to tackle. An in-depth discussion of the numerical methods for approaching population balance equations in the context of aggregation, nucleation and break-up phenomena has been developed by Kumar and Ramkrishna [11–13]. The inverse problem of population balance models, that is the mathematical approach aimed at extracting rate information from transient particle size distribution measurements, has been approached by Wright and Ramkrishna [14] for aggregation kinetics and by Sathyagal et al. [15] for particle break-up.

This article proposes a simple approach for the estimate of reaction orders in dissolution kinetics. This issue is essential in order to determine the functional dependence of the kinetic rates on the concentration of the fluid reactants.

The method proposed is based on a two-layer shrinking-core (TLSC) model, in which the effects of local surface heterogeneity and polydispersity are "lumped" together into a single parameter accounting for the increase of the surface area. Such an increase may be a consequence either of physical surface properties of solid particles or of particle polydispersity.

Albeit the model is grounded on reasonable physical approximations of the particle surface structure (see Section 3 for details), its main goal is the reaction order estimate. Therefore, this approach may become a useful tool complementing the analysis of leaching processes by means of structured models involving population balances. This approach is applied to the analysis of experimental data deriving from the dissolution of manganese oxide in an acid medium. The article is organized as follows. Section 2 briefly discusses the experimental set-up. Section 3 describes the TLSC model, its physical origin and its range of application. Throughout this article, we consider exclusively batch dissolution kinetics under the hypothesis that the fluid phase is perfectly mixed. Section 4 addresses the problem of reaction order estimate by means of the TLSC model. This problem is tackled by considering simulation results for polydisperse mixtures and, subsequently, the dissolution kinetics of $MnO_2$ particles in acid solutions in the presence of glucose.

## 2. Materials and methods

$MnO_2$ is purchased by Sigma–Aldrich (60–230 mesh, purity 99%). Leaching tests were performed in jacketed cylidrical vessels (borosilicate glass) (5 cm i.d.; 9 cm height), with round bottom and upper opening for sample collection.

Leaching experiments were carried out under magnetic stirring and thermal control was achieved through a thermostatic bath employing a circulating pump (LT5 IKA Labortechnik). The reductive leaching process was carried out in sulphuric acid medium ($H_2SO_4$ 96% ISO for analysis, Carlo Erba Reagents) using glucose (α-D-glucose

anhydrous, 96%, Sigma–Aldrich) as the reductant. The reaction fulfills the following overall stoichiometry [16]:

$$C_6H_{12}O_6 + 12MnO_2 + 24H^+ = 6CO_2 + 12Mn^{2+} + 18H_2O. \quad (2.1)$$

The experiments were performed by adding 8 g $MnO_2$ to 150 ml of solution at 90 °C, for several concentrations of the reactants (glucose, sulphuric acid). Below 90 °C, the conversion achieved after 40 h is too low to have any practical interest. During the process, different samples of liquor-leach containing solid particles were collected in order to analyze the conversion.

Solid–liquid separation was performed by centrifugation (Chermle Z380) for 10 min at speed 8000 $min^{-1}$. Liquid samples were diluted with a $HNO_3$ solution in distilled water (pH 2) and analyzed by an inductively coupled plasma spectrophotometer (ICP Varian Liberty 150) to determine the Mn concentration. Solid samples were washed with distilled water, dried at room temperature (≃20 °C) and then analyzed to determine their morphological and size properties. A morphoscopic and qualitative study of the solid particles was performed by SEM-EDS analysis (Zeiss DSM 940A): solid samples were glued to aluminium stubs, coated in a vacuum chamber with a carbon evaporation source and then analyzed.

## 3. Two-layer model

This section addresses the physical assumptions, the mathematical formulation and the range of application of the TLSC model.

For the sake of simplicity, let us assume two limiting fluid reactants under kinetics-controlled conditions (i.e. no limitations due to external mass transfer):

$$\text{solid} + \nu_1 A_1(f) + \nu_2 A_2(f) \rightarrow \text{products}. \quad (3.1)$$

These assumptions can be argumented in view of the application of this model to batch leaching of $MnO_2$ particles, which follows the overall stoichiometric balance Eq. (2.1) (further details are discussed in Section 4).

In many cases of practical interest, solid non-porous particles may exhibit surface heterogeneity properties, induced by a random distribution of the orientations of the exposed crystalline planes. This is the case of $MnO_2$ particles, as depicted in Fig. 1a and b. As it regards dissolution, the major effect of surface heterogeneity is to increase the

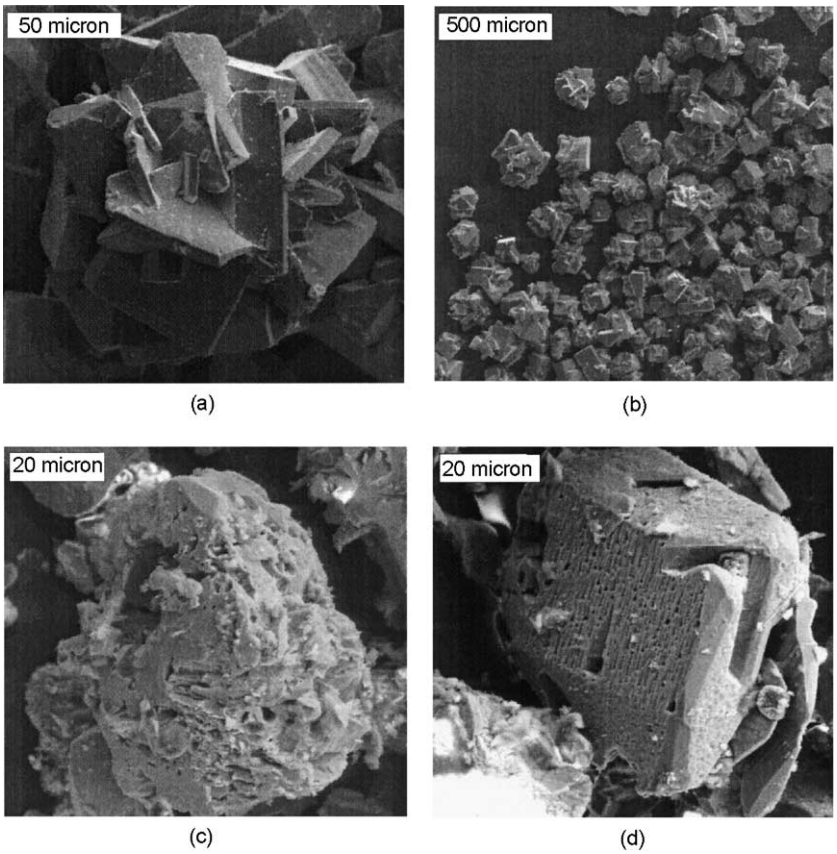


Fig. 1. SEM micrography of $MnO_2$ particles: (a and b) initial particles before leaching; (c and d) after $t = 33$ h at temperature $T = 90$ °C in the presence of an 100% surplus of glucose and sulphuric acid. The width of the white window embodied in each figure represents the reference length adopted in each micrography and is given by: (a) 50 μm; (b) 500 μm; (c and d) 20 μm.

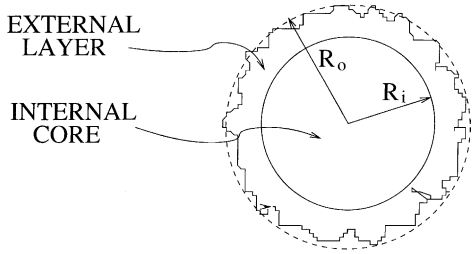


Fig. 2. Schematic representation of a solid particle in the two-layer model.

wetted surface exposed to fluid reactants, thus modifying the surface-to-volume ratio. As the reaction proceeds, sharp edges smoothen out progressively and the external particles surface becomes more regular. This phenomenon is depicted for $MnO_2$ particles in Fig. 1c and d after $t = 33$ h, during a batch leaching experiment at constant temperature $T = 90\,^{\circ}$C.

### 3.1. Model formulation

It follows from these observations that a very simple, yet physically reasonable, model accounting for the aforementioned properties can be based on the following assumptions: (i) particles are assumed to be spheres of radius $R_o$; (ii) the geometrical surface heterogeneity is accounted for by hypothesizing the presence of two layers (see Fig. 2 for a schematic pictorial description): an internal core possessing external radius $R_i$, characterized by a volume-to-surface ratio typical of regular spherical particles:

$$\frac{V(r)}{S(r)} = \frac{r}{3}, \tag{3.2}$$

and an external surface layer ($R_i < r < R_o$), characterized by a lower volume-to-surface ratio:

$$\frac{V(r)}{S(r)} = \frac{r}{3\alpha}, \tag{3.3}$$

where the constant factor $\alpha > 1$ is referred to as surface heterogeneity factor.

The assumption of spherical particles dictates that $V(r) = 4\pi r^3/3$ for $0 \le r \le R_o$. The two-layer description introduces a discontinuity at the interface between the two layers, i.e. at $r = R_i$, which needs to be eliminated through mathematical manipulations for a convenient analysis of the model. This can be achieved by assuming for the surface area scaling with $r$ a convex average between the values pertaining to the two different layers:

$$S(r) = 4\pi r^2[(1 - \phi(r; R_i, R_o)) + \alpha\phi(r; R_i, R_o)], \tag{3.4}$$

averaged with respect to a smooth function $\phi(r; R_i, R_o)$ monotonically increasing with $r$ and possessing the following properties:

$$\phi(r; R_i, R_o) = \begin{cases} 0 & \text{for } r < R_i \\ 1 & \text{for } r = R_o. \end{cases} \tag{3.5}$$

In this way, the transition between core and surface properties is modulated smoothly. A convenient choice for the weighting function $\phi$ can be the family of $c^\infty$ compactly supported functions defined by [17]:

$$\phi(r; R_i, R_o) = \begin{cases} 0 & \text{for } r \le R_i \\ \exp\left[\beta + \dfrac{\beta(R_o - R_i)^2}{(R_o - r)^2 - (R_o - R_i)^2}\right] & \text{for } R_i < r \le R_o, \end{cases} \tag{3.6}$$

where $\beta$ is a parameter, referred to as the steepness factor, controlling both the steepness of the transition between core and surface properties, and its localization around $r = R_i$. Fig. 3a shows the behavior of the ratio $rS(r)/3V(r)$ obtained from Eqs. (3.4) and (3.6) for different values of $\beta$. For values of $\beta$ significantly greater than 1, the transition from core to surface structure practically occurs for values of $r$ higher than $R_i$, thus reducing the effective width of the external layer.

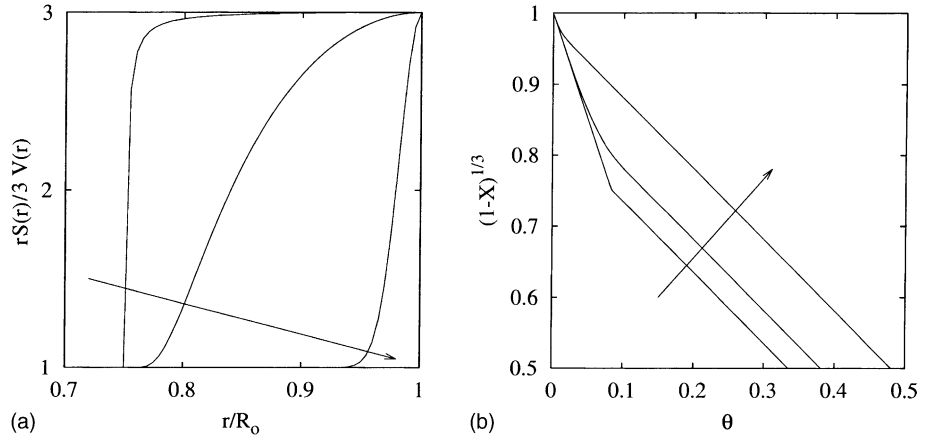


Fig. 3. (a) Behavior of the ratio $rS(r)/3V(r)$ vs. $r$ in the TLSC model at $\alpha = 3$, $R_i/R_o = 3/4$, for several values of the steepness factor $\beta = 10^{-2}, 1, 10^2$. (b) Conversion–time curves, $(1 - X(\theta))^{1/3}$ vs. $\theta$, for the TLSC model at $\alpha = 3$, $x_i = 3/4$, $\beta = 10^{-2}, 1, 10^2$. The arrow indicates increasing values of $\beta$.

Let us consider the dissolution kinetics deriving from the TLSC model, by first assuming that the fluid reactants are in large excess and that the process is under kinetics-controlled conditions. The balance equation for a generic solid particle becomes:

$$\rho_s \frac{dV(r)}{dt} = -k_d S(r). \tag{3.7}$$

By substituting Eqs. (3.4) and (3.6) and by making the equation dimensionless through the definition of the dimensionless variables: $x = r/R_o$, $\theta = tk_d/\rho_s R_o$ and $\tilde{\phi}(x; x_i) = \phi(R_o x; R_i, R_o)$, $x_i = R_i/R_o$, Eq. (3.7) becomes:

$$\frac{dx}{d\theta} = -[1 + (\alpha - 1)\tilde{\phi}(x; x_i)], \tag{3.8}$$

the solution of which is:

$$\theta = \int_x^1 \frac{dy}{[1 + (\alpha - 1)\tilde{\phi}(y; x_i)]}. \tag{3.9}$$

Fig. 3b shows the dimensionless conversion–time curves[1] $(1 - X)^{1/3}$ versus $\theta$, where $X = 1 - x^3$, obtained from Eq. (3.9) for several values of $\beta$. The TLSC model has been built so as to provide a crossover behavior in the conversion–time curves: from surface-controlled shrinking, enhanced by the increase in the surface area within the external region, i.e. for $x > x_i$, to the core-controlled dissolution. These two regimes correspond to a linear scaling of the conversion versus time, characterized by a slope equal to $\alpha$ and 1, respectively. This phenomenon is evident for values of $\beta \leq 1$, whereas for $\beta \gg 1$ the effects of surface heterogeneity become less pronounced. This is a consequence of the fact that the effective region of surface heterogeneity shifts towards higher values of $x$ beyond $x_i$, as depicted in Fig. 3a, so that the effective width of the external layer is significantly reduced.

To sum up, the TLSC model contains three adjustable parameters, $\alpha$, $\beta$ and $x_i$ that modulate the effects of the particle surface heterogeneity and the transition from internal (core) to surface structure.

The analysis can be extented to the case where the fluid reactants are not in large excess. In this situation, the dissolution rate depends explicitly on the conversion. For example, let us suppose that the rate of dissolution (mass of solid dissolved per unit time and unit wetted area) may be expressed as:

$$\omega(c_1, c_2) = -k_0 c_1^{n_1} c_2^{n_2}, \tag{3.10}$$

where $c_i$ $(i = 1, 2)$ are the concentrations of the fluid reactants and $n_1$, $n_2$ are positive exponents. The stoichiometric balance associated with Eq. (3.1) dictates that:

$$c_i(t) = c_{s,0}[\gamma_i \nu_i - \nu_i X(t)], \tag{3.11}$$

where $c_{s,0} = n_{s,0}/V_r$ is the molar concentration of the solid reactant referred to the reactor volume and $\gamma_i = c_i(0)/c_{s,0}\nu_i$ $(i = 1, 2)$ account for the loading ratio of the $i$th fluid reactant to the solid. In the case of shrinking-core models the conversion is expressed by $X = 1 - x^3$, the dimensionless time $\theta$ should be defined as $\theta = tk_0 c_{s,0}^{n_1+n_2}/\rho_s R_o$ and the formal solution of the balance equation is given by:

$$\theta = \int_x^1 \left\{ \prod_{i=1}^{2} [\gamma_i \nu_i - \nu_i (1 - y^3)]^{n_i} \right\}^{-1} \frac{dy}{1 + (\alpha - 1)\tilde{\phi}(y; x_i)}. \tag{3.12}$$

### 3.2. Application of TLSC: general observations

The understanding of dissolution phenomena and their optimization in process units is intrinsically connected to the development of structured models in which the polydispersity of the solid particle ensemble and the physico-chemical/mechanical processes (that is the interplay between dissolution and fragmentation) are explicitly accounted for.

It follows from this general observation that, notwithstanding its physical motivations, the exclusive use of the TLSC model solely as a slightly more elaborate shrinking-core model would be of limited practical and conceptual usefulness. Consequently, the TLSC model should be implemented within the main street of population balance models. In order to explore this point in more detail, let us begin with an experimental observation. Fig. 7A depicts[2] several typical conversion–time curve for $MnO_2$ particles obtained at $T = 90\,^{\circ}C$ under different operating conditions, i.e. different surplus[3] of glucose and of sulphuric acid. As can be observed, the conversion–time curve displays a crossover behavior similar to that characterizing the TLSC model: to an initial linear behavior for $X < X^*$ (with $X^* \simeq 0.2 \div 0.5$), an "almost" linear scaling, characterized by a less steep slope, follows. This phenomenology is due to a manifold of concurring phenomena: (i) the surface structure of the solid particles (see Fig. 1); (ii) the polydisperse nature of the solid particle mixture, (iii) fragmentation processes; (iv) kinetic effects deriving from the consumption of limiting reactants.

All these phenomena find a mathematical description[4] in the population balance equation Eq. (1.1). The

[1] Throughout this article, we prefer to represent the conversion–time curves as $(1-X)^{1/3}$ versus time. This is due to graphical reasons, in order to emphasize the crossover behavior occurring at short and intermediate timescales, and the linear behavior characteristic of shrinking-core models in reaction-controlled regime.

[2] A detailed discussion on the experimental conditions for $MnO_2$ dissolution is developed in Section 4.

[3] The concept of "surplus" of a fluid reactant is referred to its molar content with respect to the stoichiometric loading, which corresponds to a molar ratio of the fluid to solid reactant equal to the ratio of the corresponding stoichiometric coefficients.

[4] This observation holds true for the dissolution of homogeneous particles, as in the case considered in this article for pure $MnO_2$. In the case of ore leaching, a detailed mathematical formulation of the dissolution process may be more complex due to the presence of the reactant and of inert solid. The spatial distribution of reactant crystallites within a solid particle should be accounted for, e.g. by means of generalized grain models.

qualitative resemblance of the experimental and TLSC model conversion–time curves (Fig. 3b and Fig. 7A) suggests that TLSC model might be used for a lumped description of dissolution kinetics, in which model parameters $\alpha$, $\beta$ and $x_i$ encompass surface properties of the solid particles and/or polydispersity features, such as the variability of the effective surface area with time during the dissolution process.

In the presence of a significant distribution of fines, either initially present or generated during the dissolution/fragmentation dynamics, the effects of polydispersity on the overall quantities (such as conversion), can be approximated by means of a "mean" particle possessing surface heterogeneity properties as described within the TLSC model.

The intensive parameters (e.g. the reaction orders), which are less sensitive to the structural properties of solid particles and of the particle distribution function, can be thus estimated within the framework of the TLSC model, in a fairly objective way, independently of the lumping approach characterizing this approximation.

Specifically, the main goal of this article is to show that the TLSC model may provide an accurate estimate of the functional dependence of the dissolution rates on the concentration of the fluid reactants. This is the subject of Section 4.

## 4. Data analysis and results

This section addresses how the TLSC model can be applied for reaction order estimate, that is, for the identification of the functional dependence of the dissolution kinetics on the concentration of the fluid reactants. First, we formulate the problem and support the analysis with model results. Subsequently, we apply this approach to the dissolution of $MnO_2$ particles.

### 4.1. Statement of the problem and model results

Let us consider a polydisperse solid mixture, by overlooking the effects of fragmentation,[5] i.e. is by assuming $a(r) = 0$ in Eq. (1.1) and by assuming a functional dependence of the dissolution rate $\omega$ given by Eq. (3.10). The overall conversion is given by:

$$X(t) = 1 - \frac{\int_0^\infty r^3 n(r,t)\,\mathrm{d}r}{\int_0^\infty r^3 n_0(r)\,\mathrm{d}r} = 1 - \frac{N_3(t)}{N_3(0)}, \tag{4.1}$$

where $n_0(r) = n(r, t = 0)$ is the initial particle distribution. Due to the explicit dependence of $\omega$ on the concentration of the fluid reactants, the dissolution rate becomes a non-linear functional of the particle distribution function, through its dependence on the third-order moment:

$$\omega[r, N_3(t)] = -k_0 c_{\mathrm{s},0}^{n_1+n_2} \prod_{i=1}^{2} \left[\gamma_i \nu_i - \nu_i \left(1 - \frac{N_3(t)}{N_3(0)}\right)\right]^{n_i} = -k_\mathrm{d}\omega_0[N_3(t)]. \tag{4.2}$$

Let us assume that the initial distribution is bounded from above, i.e. $n_0(r) = 0$ for $r > R_{\max}$. By introducing the variables $x = r/R_{\max}$, $\theta = tR_{\max}/k_\mathrm{d}$, Eq. (1.1) takes the dimensionless form:

$$\frac{\partial n(x,\theta)}{\partial \theta} + \frac{\partial}{\partial x}\{\omega_0[N_3(\theta)]n(x,\theta)\} = 0, \tag{4.3}$$

where we have used the same notation $n(x, \theta)$ to indicate the dimensionless particle distribution function depending on the dimensionless variables $x$ and $\theta$.

Let us consider a first-order reaction with respect to $A_1$, that is $n_1 = 1$, $n_2 = 0$, with $\nu_1 = 1/12$. This value of $\nu_1$ corresponds to the overall reaction Eq. (2.1), by identifying $A_1$ as glucose and by assuming that the dissolution rate does not depend on the concentration of sulphuric acid. In order to highlight the effects of polydispersity and the role of fines, let us consider the following initial bimodal distribution (Fig. 4):

$$n_0(x) = Ax(1-x)[\exp(-a_1(x-x_1)^2) + c_2\exp(-a_2(x-x_2)^2)], \qquad x \in [0,1], \tag{4.4}$$

where $a_1 = a_2 = 10^3$, $x_1 = 0.1$, $x_2 = 0.8$, $c_2 = 2 \times 10^{-3}$ and $A$ is an arbitrary normalization constant that does not affect the conversion–time curves.

The bimodal nature of the initial mass distribution function $x^3 n_0(x)$ foresees the occurrence of a crossover behavior in the conversion–time curves, Fig. 5, apparently similar to that observed in Fig. 3b in the case of TLSC model and in Fig. 7A for $MnO_2$ dissolution. The origin of this crossover phenomenon has no relation with the physical assumptions

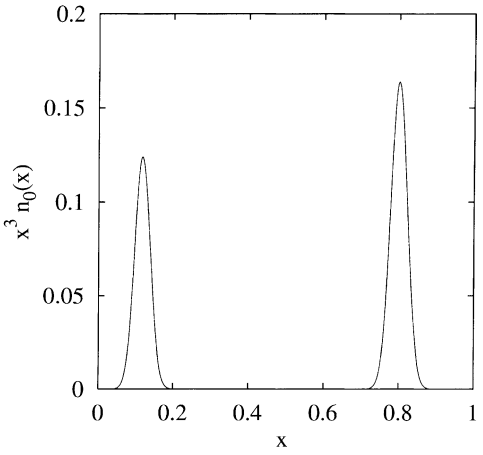


Fig. 4. Normalized initial mass distribution $x^3 n_0(x)$ vs. $x$, Eq. (4.4) ($A = 10^3$).

[5] The inclusion of fragmentation processes can be straightforwardly performed without any significant change in the present analysis oriented towards reaction order estimate.

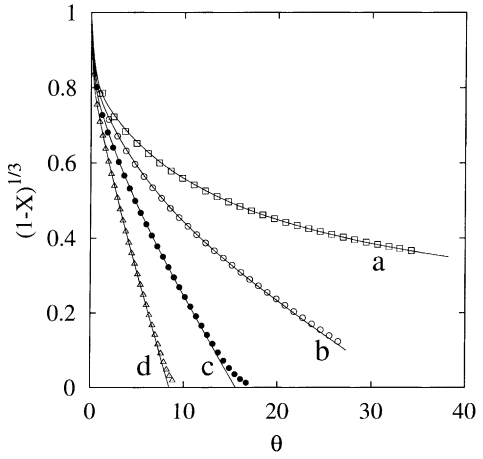


Fig. 5. Conversion–time curve $(1 - X(\theta))^{1/3}$ vs. $\theta$ for the model system obtained in the presence of a first-order kinetics $\nu_1 = 1/12$, starting from the initial particle distribution Eq. (4.4): (□) $\gamma_1 = 1$; (○) $\gamma_1 = 1.2$; (●) $\gamma_1 = 1.5$; (△) $\gamma_1 = 2$. Solid lines are the corresponding predictions of the TLSC model for $n_1 = 1$.

underlying the TLSC model, as it can be entirely attributed to the polydispersity of the particle ensemble. In principle, the behavior of the effective surface, induced by mixture polidispersity, can be accounted for within the TLSC model by means of the model expression Eq. (3.4) through a suitable choice of the parameters $\alpha$, $\beta$ and $x_i$. Besides, kinetic effects, that is the influence of the functional form of the dissolution rate, can be obtained through a quantitative analysis for an objective[6] parameter estimation. This is the reason why this physical setting may be regarded as a valid test case in order to check quantitatively the effective ability of the TLSC model to estimate the order of reaction in the presence of a continuous distribution of particle sizes.

It follows that parameter estimation should be performed in such a way as to single out the kinetic effects, i.e. the functional form of the dissolution rate, as much as possible. This is the reason why we adopt a mixed regressive–predictive optimization procedure. Let us suppose, we collect an ensemble of experimental data curves for different values of the loading ratio $\gamma_1$ of the limiting reactant and let us take one of the ensemble curve at $\gamma_1 = \gamma_1^*$ as the reference curve. For any functional form of the dissolution rate, TLSC model parameters are optimized in order to achieve the optimal regression of the reference curve at $\gamma_1^*$ (regression step). With the value of the TLSC parameter thus obtained, the other conversion–time curves are predicted (prediction step), and kinetic parameters (e.g. the order of reaction) are optimized by referring to the prediction properties for $\gamma_1 \neq \gamma_1^*$.

Specifically, the numerical test is performed as follows. Numerical data are generated through the solution of Eq. (4.3) for different values of the loading ratio ($\gamma_1 =$ 1, 1.2, 1.5, 2.0) corresponding to stoichiometric loading conditions ($\gamma_1 = 1$) and to a surplus of 20, 50 and 100% of the fluid reactant. Eq. (4.3) can be solved in closed form by making use of the warped-time transformation developed in [18]. The resulting conversion–time curves are depicted in Fig. 5 and are used as synthetic "experimental" data. These data are fitted by means of the TLSC model, by assuming Eq. (3.10) with $n_2 = 0$ as the kinetic model, for different values of the order of reaction $n_1$. The regression step proceeds as follows: for each value of $n_1$, the values of the parameters $\alpha$, $\beta$ and $x_i$, characterizing the TLSC model, are estimated by means of standard optimization methods in order to obtain the optimal regression against the synthetic experimental data corresponding to 100% surplus ($\gamma_1 = 2$). The TLSC model with the value of the parameters thus obtained (for each value of $n_1$) is used to predict the behavior of the "experimental" conversion–time curve for the other operating conditions ($\gamma_1 = 1$, 1.2, 1.5).

The results of the regression ($\gamma_1 = 2$) and of the predictions ($\gamma_1 = 1$, 1.2, 1.5) of the TLSC model are depicted in Fig. 5 as solid lines for $n_1 = 1$. For $n_1 = 1$, that is, for the correct value of the reaction order, the TLSC model is able to predict accurately the overall reaction evolution for all the operating conditions considered.

It is useful to obtain a quantitative representation of the distance between the "experimental" data and TLSC model predictions as a function of $n_1$. This is depicted in Fig. 6, by expressing the distance as:

$$d(n_1; \gamma_1) = \left\{ \frac{1}{\theta_{\max}} \int_0^{\theta_{\max}} [y_{\exp}(\theta; \gamma_1) - y_{\mathrm{TL}}(\theta; n_1, \gamma_1)]^2 \, \mathrm{d}\theta \right\}^{1/2}, \tag{4.5}$$

where $y_{\exp}(\theta; \gamma_1) = (1 - X_{\exp}(\theta; \gamma_1))^{1/3}$ are the "experimental" data of the conversion–time behavior for a value $\gamma_1$ of the loading ratio, and $y_{\mathrm{TL}}(\theta; n_1; \gamma_1)$ the corresponding

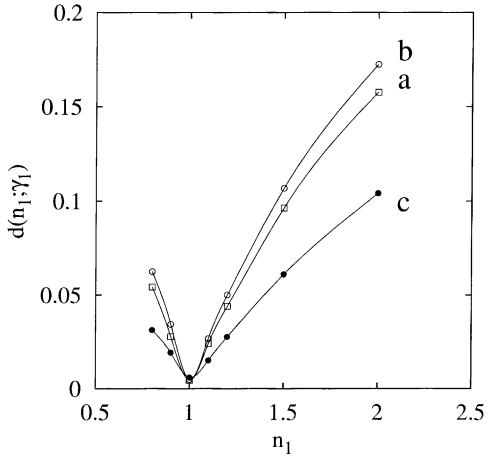


Fig. 6. Distance function $d(n_1; \gamma_1)$ vs. $n_1$ for different loading ratios: (a) $\gamma_1 = 1$; (b) $\gamma_1 = 1.2$; (c) $\gamma_1 = 1.5$.

[6] In this context the wording "objective" refers to an estimate of the kinetic rates indepedent of the biasing effects deriving from solid particle polydispersity.

predictions of the TLSC model for the same loading ratio and for a value $n_1$ of the reaction order. The model predictions are obtained as discussed above, that is by estimating model parameters from the case $\gamma_1 = 2$.

The distance function $d(n_1; \gamma_1)$ defined by Eq. (4.5) contains an additional parameter $\theta_{max}$ corresponding to the time windows over which the comparison is performed. The value of $\theta_{max}$ is chosen equal to 15, 25 and 35 for $\gamma_1 = 1$, 1.2 and 1.5, respectively. As can be observed from Fig. 6, the distance function shows a local and absolute minimum for $n_1 = 1$, that is at the correct value of the reaction order $n_1$ corresponding to the synthetic "experimental" data. This is a clear quantitative indication that the TLSC model can be successfully applied as a shortcut approach for identifying the functional dependence of the dissolution rate on the concentration of the fluid reactants in the presence of a polydisperse ensemble of solid reacting particles.

### 4.2. Application to the $MnO_2$ dissolution kinetics

The recovery of metals and particularly of manganese from mineral ores is an important industrial issue. A series of hydrometallurgical processes has been developed both with and without reducing agents. One of the processes developed makes use of sacchariferous reductant (glucose in the present analysis). Recently, bioleaching of manganese by iron-oxidizing bacteria have been addressed [19,20]. Leaching kinetics of manganiferous ore (pirolusite) have been considered by several authors [21,22].

Manganese extraction using carbohydrates as reducing agents consists of a complex network of chemical reactions involving partially oxidized products derived from carbohydrate degradation in acidic media. The manifold of intermediates and their variability with carbohydrate source led to the formulation of a preliminary kinetic model considering the overall chemical reaction Eq. (2.1), thus overlooking all the possible intermediate products and reactions. A shrinking-core model with a variable activation energy (the activation energy is assumed to be a function of the overall conversion) was developed in [23]. This model is able to fit successfully the experimental data of manganese ore leaching obtained at different operating conditions [24], albeit the functional form of the dissolution rate is rather complex and the model contains many adjustable parameters.

A thorough understanding of ore leaching kinetics is made complex by the structural properties of the particles and by the spatial distribution of $MnO_2$ crystallites within the amorphous solid matrix. In order to achieve a better understanding of the kinetics underlying the reaction described by Eq. (2.1), it is useful to consider the leaching process of pure $MnO_2$ particles. The reaction is carried out in acidic medium and glucose is used as the reducing agent. The overall stoichiometry of the reaction is described by Eq. (2.1).

This section analyzes the kinetics of this reaction by applying the TLSC model for the estimate of the functional dependence of the dissolution rate on glucose and sulphuric acid concentrations. We indicate with subscript "1" glucose and with subscript "2" sulphuric acid, so that $\gamma_1$ is the loading ratio of glucose to the solid reactant.

Let us first consider the influence of sulphuric acid. Experimental data indicate that the overall dissolution rate depends very weakly on the concentration of $H_2SO_4$. Fig. 7A shows the experimental results at $T = 90\,^{\circ}C$ for several loading conditions: under stoichiometric loading for glucose ($\gamma_1 = 1$), by keeping sulphuric acid under stoichiometric loading ($\gamma_2 = 1$) and in the case of a 30% surplus ($\gamma_2 = 1.3$) (data set a); for 50% glucose surplus ($\gamma_1 = 1.5$), under stoichiometric ($\gamma_2 = 1$) and 50% surplus ($\gamma_2 = 1.5$) of sulphuric acid (data set b). As can be observed (experimental data sets a and b in Fig. 7A), a surplus of sulphuric acid, the other operating parameters being fixed, does not increase

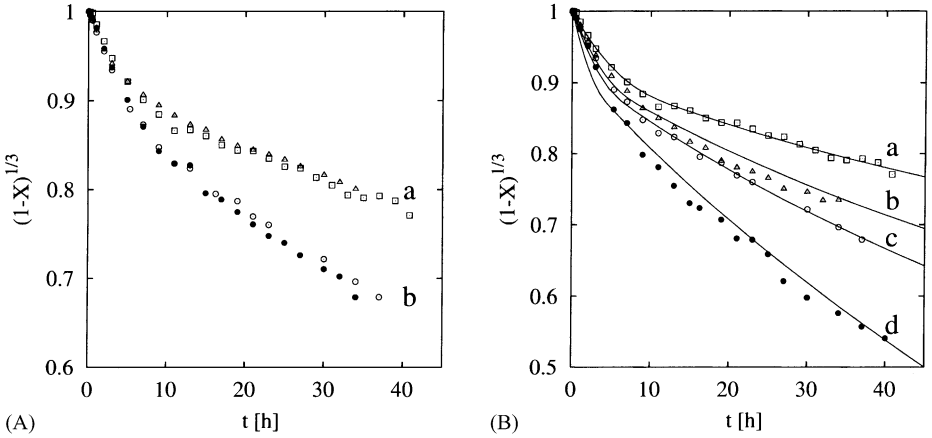


Fig. 7. (A) Influence of sulphuric acid concentration on the dissolution of $MnO_2$. Conversion–time curves $(1-X(t))^{1/3}$ vs. $t$. Set (a) refers to stoichiometric loading conditions of glucose $\gamma_1 = 1$, (□) to stoichiometric loading of sulphuric acid $\gamma_2 = 1$ and (△) to 30% surplus of sulphuric acid $\gamma_2 = 1.3$. Set (b) refers to 50% glucose surplus $\gamma_1 = 1.5$, (●) to stoichiometric loading of sulphuric acid $\gamma_2 = 1$ and (○) to 50% surplus of sulphuric acid $\gamma_2 = 1.5$. (B) Influence of glucose concentration on the dissolution of $MnO_2$. Conversion–time curves $(1 - X(t))^{1/3}$ vs. $t$: (□) $\gamma_1 = 1$; (△) $\gamma_1 = 1.3$; (○) $\gamma_1 = 1.5$; (●) $\gamma_1 = 2$. Solid lines are the prediction of the TLSC model for $n_1 = 1.2$.

the overall conversion so that, for pure $MnO_2$, it can be reasonably assumed that the dissolution rate is independent of the concentration $c_2$ of $H_2SO_4$.

The influence of glucose on the overall reaction kinetics is more pronounced (Fig. 7B): an increase of the glucose loading ratio $\gamma_1$ speeds up the overall conversion, thus indicating that the dissolution rate depends on glucose concentration.

Data analysis has been performed following the same procedure outlined in the previous subsection: model parameters of TLSC are optimized with respect to the experimental data set corresponding to a reference case, corresponding to the stoichiometric loading conditions ($\gamma_1 = 1$, $\gamma_2 = 1$) and, subsequently, the TLSC model is applied to predict the conversion–time curves corresponding to the other operating conditions.

For the dissolution rate we assume a simple functional dependence on glucose concentration:

$$\omega(c_1, c_2) = -k_0 c_1^{n_1}, \tag{4.6}$$

where $n_1$ is the parameter to be estimated. Fig. 8 shows the behavior of the distance function $d(n_1; \gamma_1)$, Eq. (4.5), versus $n_1$ for $\gamma_1 = 1.3$ and $\gamma_1 = 2$. For $\gamma_1 = 1.3$ (curve a of Fig. 8), there exists a broad range of values $1 < n_1 < 1.6$ for which the predictions of the TLSC model are in acceptable agreement with the experimental data. Conversely, the case of a 100% surplus of glucose (curve b) of Fig. 8 clearly indicates the occurrence of a local and absolute minimum at $n_1 = 1.2$. The solid lines depicted in Fig. 7B refer to the TLSC model prediction in the presence of a dissolution rate given by Eq. (4.6) with $n_1 = 1.2$ (the values of the other parameters are $\alpha = 3$, $\beta = 1$, $\rho_s R_{max}/k_0 c_{s,0}^{1.2} = 7.8\,h$, $x_i = 0.85$). The agreement is satisfactory and this is a further confirmation of the ability of TLSC model to extract quantitative information about dissolution rates.

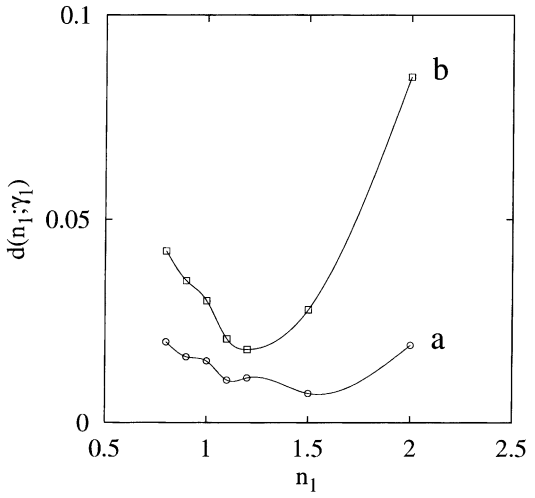


Fig. 8. Distance function $d(n_1; \gamma_1)$ vs. $n_1$ for different loading ratios in the case of $MnO_2$ dissolution: (a) $\gamma_1 = 1.3$; (b) $\gamma_1 = 2$.

## 5. Concluding remarks

The aim of this article is to develop a simple method for the estimate of the functional dependence of the dissolution rate on the concentration of the fluid reactants, by means of a modified version of the shrinking-core model, i.e. the TLSC model. TLSC model has been developed to provide a simple approach to experimental batch dissolution kinetics, characterized by two almost linear slopes in the conversion–time curves.

TLSC is a fairly flexible model characterized by three adjustable parameters, $\alpha$, $\beta$ and $x_i$, related to the surface heterogeneity of solid particles. The model can be successfully applied to mimic the overall kinetic behaviour during the dissolution of polydisperse particle mixtures.

The main results of this article can be summarized as follows: (i) TLSC model is a simple model accounting for local surface heterogeneity of solid particles; (ii) this model provides a flexible tool for estimating the order of reaction in dissolution kinetics.

In this framework, a conceptual observation should be pointed out neatly. Albeit the analysis performed either on model systems or experimental data indicate that TLSC is able to predict the overall reaction kinetics in a variety of conditions involving polydisperse systems, we believe that its main application should be limited to a processing tool for estimating the reaction orders and more generally the functional form of the dissolution rate. The latter application of TLSC model should be performed in close connection with structured models for the evolution of a polydisperse ensemble of solid particles which encompass the main physical properties (polydispersity, etc.) and phenomenologies (interplay between dissolution and fragmentation) characterizing leaching processes in laboratory and industrial equipments.

Following this approach, the TLSC model has been applied to the dissolution kinetics of $MnO_2$ particles, revealing that the dissolution rate is substantially independent of the concentration of sulphuric acid and can be modeled by means of a fractional-order kinetics with $n_1 = 1.2$ with respect to glucose. This is a first step towards the development of a structured model for $MnO_2$ and manganiferous ore dissolution, that will be developed elsewhere by means of population balance equations.

## References

[1] C.Y. Wen, Non-catalytic heterogeneous solid–fluid reaction models, Ind. Eng. Chem. 60 (1969) 34.
[2] H.Y. Sohn, M.E. Wadsworth, Rate processes of extractive metallurgy, Plenum Press, New York, 1979.
[3] J.E. Sepulveda, J.A. Herbst, A population balance approach to the modelling of multistage continuous leaching systems, AIChE Symp. Ser. 57 (1978) 41.
[4] W.W. Stange, R.P. King, L. Woollacott, Towards more effective simulation of CIP and CIL processes. Part 2. A population balance-based

simulation approach, J. S. Afr. Inst. Miner. Metall. 90 (1990) 307.
[5] F.K. Crundwell, A.W. Bryson, The modelling of particulate leaching reactors—the population balance approach, Hydrometallurgy 29 (1992) 275.
[6] S.E. Le Blanc, H.S. Fogler, Population balance modeling of the dissolution of polydisperse solids: rate-limiting regimes, AIChE J. 33 (1987) 54.
[7] S.E. Le Blanc, H.S. Fogler, Dissolution of powdered minerals: the effect of polydispersity, AIChE J. 35 (1989) 865.
[8] B.F. Edwards, M. Cai, H. Han, Rate equation and scaling for fragmentation with mass loss, Phys. Rev. A 41 (1990) 5755.
[9] M. Cai, B.F. Edwards, H. Han, Exact and asymptotic scaling solutions for fragmentation with mass loss, Phys. Rev. A 43 (1991) 656.
[10] D. Ramkrishna, The status of population balances, Rev. Chem. Eng. 3 (1985) 59.
[11] S. Kumar, D. Ramkrishna, On the solution of population balance equations by discretization. Part I. A fixed pivot technique, Chem. Eng. Sci. 51 (1996) 1311.
[12] S. Kumar, D. Ramkrishna, On the solution of population balance equations by discretization. Part II. A moving pivot technique, Chem. Eng. Sci. 51 (1996) 1333.
[13] S. Kumar, D. Ramkrishna, On the solution of population balance equations by discretization. Part III. Nucleation, growth and aggregation of particles, Chem. Eng. Sci. 52 (1997) 4659.
[14] H. Wright, D. Ramkrishna, Solutions of inverse problems in population balances. Part I. Aggregation kinetics, Comput. Chem. Eng. 16 (1992) 1019.
[15] A.N. Sathyagal, D. Ramkrishna, G. Narsimhan, Solution of inverse problems in population balances. Part II. Particle break-up, Comput. Chem. Eng. 19 (1995) 437.
[16] F. Veglió, L. Toro, Reductive leaching of a concentrate manganese dioxide ore in acid solution: stoichiometry and preliminary kinetic analysis, Int. J. Miner. Process. 40 (1994) 257–272.
[17] V.S. Vladimirov, Equations of mathematical physics, Mir, Moscow, 1984.
[18] M. Giona, A. Adrover, F. Pagnanelli, L. Toro, A closed-form solution of population balance models for the dissolution of polydisperse mixtures, Chem. Eng. J., in press.
[19] T. Kai, Y.I. Suenaga, A. Migita, T. Takahashi, Kinetic model for the simultaneous leaching of zinc sulfide and manganese dioxide in the presence of iron-oxidizing bacteria, Chem. Eng. Sci. 55 (2000) 3429.
[20] F. Veglió, F. Beolchini, A. Nardini, L. Toro, Bioleaching of pyrrhotite ore by sulfoxidans strain: kinetic analysis, Chem. Eng. Sci. 55 (2000) 783.
[21] Z. Ma, C. Ek, Rate processes and mathematical modelization of the acid leaching of a manganese carbonate ore, Hydrometallurgy 27 (1991) 125.
[22] Z. Ma, C. Ek, Engineering application of the acid leaching kinetics of a manganese carbonate ore, Hydrometallurgy 28 (1992) 223.
[23] M.I. Brittan, Variable activation energy model for leaching kinetics, Int. J. Miner. Process. 2 (1975) 321.
[24] F. Veglió, M. Trifoni, F. Pagnanelli, L. Toro, Shrinking-core model with variable activation energy: a kinetic model of manganiferous ore leaching with sulphuric acid and lactose, Hydrometallurgy 60 (2001) 167.